Carbohydrate Research xxx (2014) xxx–xxx

Contents lists available at ScienceDirect

Carbohydrate Research

journal homepage: www.elsevier.com/locate/carres

Comparison of separation techniques for the elucidation of IgG N-glycans pooled from healthy mammalian species

Barbara Adamczyk[a,b,†], Tharmala Tharmalingam-Jaikaran[a,†,‡], Michael Schomberg[a,§], Ákos Szekrényes[c], Ronan M. Kelly[a,¶], Niclas G. Karlsson[b], Andràs Guttman[c,d], Pauline M. Rudd[a,*]

[a] GlycoScience Group, NIBRT–The National Institute for Bioprocessing Research and Training, Fosters Avenue, Mount Merrion, Blackrock, Co. Dublin, Ireland
[b] Medical Biochemistry, University of Gothenburg, Gothenburg, Sweden
[c] Horváth Laboratory for Bioseparation Sciences, Research Center for Molecular Medicine, University of Debrecen, 4032 Debrecen, Hungary
[d] MTA-TKI Translational Glycomics Research Group, University of Pannonia, Veszprem, Hungary

ARTICLE INFO

Article history:
Received 9 November 2013
Received in revised form 13 January 2014
Accepted 23 January 2014
Available online xxxx

Keywords:
Protein glycosylation
IgG
Glycan analysis
HILIC–UPLC
RP–UPLC
CE-LIF

ABSTRACT

The IgG N-glycome provides sufficient complexity and information content to serve as an excellent source for biomarker discovery in mammalian health. Since oligosaccharides play a significant role in many biological processes it is very important to understand their structure. The glycosylation is cell type specific as well as highly variable depending on the species producing the IgG. We evaluated the variation of N-linked glycosylation of human, bovine, ovine, equine, canine and feline IgG using three orthogonal glycan separation techniques: hydrophilic interaction liquid chromatography (HILIC)–UPLC, reversed phase (RP)–UPLC and capillary electrophoresis with laser induced fluorescence detection (CE-LIF). The separation of the glycans by these high resolution methods yielded different profiles due to diverse chemistries. However, the % abundance of structures obtained by CE-LIF and HILIC–UPLC were similar, whereas the analysis by RP-UPLC was difficult to compare as the structures were separated by classes of glycans (highly mannosylated, fucosylated, bisected, fucosylated and bisected) resulting in the co-elution of many structures. The IgGs from various species were selected due to the complexity and variation in their N-glycan composition thereby highlighting the complementarity of these separation techniques.

1. Introduction

Oligosaccharides play a significant role in the bioactivity, stability and functionality of serum proteins such as IgG.[1] Each heavy chain of IgG has an N-glycan covalently linked at the highly conserved Asn[297] of the Fc region of the molecule; as well, 15–20% of normal polyclonal IgG molecules bear N-linked oligosaccharides in the variable (V) regions of the light (L) and/or heavy (H) chains.[2] Since glycosylation is species and cell type specific, IgGs produced in different host mammals contain different oligosaccharide patterns. The glycan heterogeneity is a reflection upon the presence and lifetime of glycosyltransferases in the Golgi of the different species of mammals.[3]

Glycosylation of proteins is critical for biological function, and consequently the analysis of this post translational modification is ultimately important. With the advancement in novel technologies, there are several methods available for the high-throughput separation and analysis of glycans. Rapid analysis methods are beneficial for high throughput; however, results may vary depending on the separation technique selected. Current techniques for profiling, characterization and analysis of glycans include hydrophilic liquid chromatography (HILIC),[4–7] reverse phase chromatography (RP),[8,9] capillary electrophoresis (CE),[10–12] mass spectrometry (MS),[13–17] nuclear magnetic resonance (NMR) [18,19] amongst others.

Since oligosaccharides have no appreciable photometric properties, sensitive detection requires labelling the glycans with a

Abbreviations: 2-AB, aminobenzamide; 2-AMAC GA, 2-aminoacridone labelled glucuronic acid; ABS, *Arthrobacter ureafaciens* sialidase; APTS, 8-aminopyrene-1,3,6-trisulfonic acid; AU, arabinose units; BKF, bovine kidney alpha-fucosidase; BTG, bovine testes beta-galactosidase; CE, capillary electrophoresis; CE-LIF, capillary electrophoresis with laser induced fluorescence; GU, glucose units; GU_{CE}, glucose units (capillary electrophoresis); GUH, hexosaminidase cloned from *Streptococcus pneumoniae* expressed in *E. coli*; HILIC, hydrophilic liquid chromatography; HSS, high strength silica; IgG, immunoglobulin G; MS, mass spectrometry; Neu5Ac, *N*-acetylneuraminic acid; Neu5Gc, *N*-glycolylneuraminic acid; NMR, nuclear magnetic resonance; PNGaseF, recombinant peptide-N-glycosidase-F; RP, reversed phase; UPLC, ultra performance liquid chromatography.

* Corresponding author. Tel.: +353 12158142; fax: +353 12158116.
E-mail address: pauline.rudd@nibrt.ie (P.M. Rudd).
† These authors contributed equally to this work.
‡ Current address: Amgen Inc., Thousand Oaks, CA, USA.
§ Current address: Max-Planck Institute for Dynamics of Complex Technical Systems, Magdeburg, Germany.
¶ Current address: Eli Lilly S.A., Irish Branch, Kinsale, Co. Cork, Ireland.

http://dx.doi.org/10.1016/j.carres.2014.01.018
0008-6215/

fluorescent tag. The HILIC separation of 2-aminobenzamide (2AB) labelled glycans, which is based on the hydrophilic interaction between the analyte and the stationary phase, is well characterized and understood.[7] The technology is robust, uses minimal glycoprotein material and the technology has been optimized to enable short separation times.[7,20,21] The fluorescence detection is sensitive, allowing for detection of femtomolar concentrations.[22] HILIC separation is based on a polar stationary phase and a non-polar mobile phase.[23] On the contrary, reverse phase separation is based on hydrophobicity and thus utilizes a non-polar stationary phase and a polar mobile phase where glycans are eluted by increasing concentrations of organic solvent.

CE-LIF has proven to be a sensitive and high resolution separation method that is already broadly utilized in the analysis of complex carbohydrates, both by the biomedical as well as the biotechnology industries.[24–26] CE separation is driven by an electric field mediated migration and is therefore based on charge to hydrodynamic volume ratio. Highly charged species migrate first. Additional structural information can be obtained when this electrophoretic separation technique is combined with exoglycosidase-array mediated sequencing.[27] The selection of the label can have a profound effect on both the sensitivity and resolving power of the method.[25] The ideal labelling agent for CE provides easy and fast glycan derivatization but also has high quantum yield, sufficient charge properties and an excitation wavelength that fits for commercially available lasers. The most commonly used fluorophore which meets these criteria is 8-aminopyrene-1,3,6-trisulfonic acid (APTS).[24,28]

For each of the selected separation techniques peak retention/migration times are directly correlated to a standard oligosaccharide ladder used to allow for initial structural assignment of the glycans of interest. The choice of the ladder depends on the matrix by which the separation occurs. In case of HILIC the sugar ladder consists of glucose units linked via an α1,6 linkage (dextran) with a 2AB label at the reducing end, in RP it consists of L-arabinose units linked via an α1,5 linkage (arabinose ladder) also 2AB labelled, and in CE, APTS derivatized maltodextrin is used for structural assignment (glucose units linked via an α1,4 linkage).[29] In either separation mechanism, each sugar chain oligomer has a distinct retention/migration time. By correlation of the retention/migration time and length of the sugar oligomer a calibration is generated to assign GU (glucose units), AU (arabinose units) and GU_{CE} (glucose units for capillary electrophoresis) values to unknown oligosaccharides. Furthermore, with databases such as Glycobase,[30,4] we are able to assign the most probable structures to separated glycans. The digestion of glycans from the non-reducing ends via use of exoglycosidase enzymes allows for further confirmation of the suggested structures and the determination of the sequence, anomericity and linkage of different sugars to the core structure.

In this paper we investigated three glycan separation methods using the N-glycans from the IgGs of human, bovine, ovine, equine, canine and feline origin. Samples were treated with peptide-N-glycosidase-F (PNGase F), and the released oligosaccharide structures were analysed by three orthogonal glycan separation techniques: HILIC–UPLC, RP–UPLC and CE-LIF. The methods took advantage of different chemistries, and thus should reflect the different attributes present in the IgG glycans. The IgGs from these various species were selected because of their complexity and variation in *N*-glycan composition to highlight the complementarity of these separation techniques.

2. Materials and methods

2.1. Materials

Human and ovine IgGs were obtained from Sigma-Aldrich (St. Louis, MO), while bovine ($n = 12$), equine ($n = 10$), canine ($n = 8$) and feline ($n = 8$) serum samples were obtained from UCD Veterinary Sciences. Samples were collected on the admission of the animal to the veterinary clinic for biochemical measurements, they were stored in −80 °C and upon confirmation of healthy status they were transferred for IgG purification and glycan analysis. A representative pool for each species was prepared by pooling all individual subjects.

2.2. Chemicals and reagents

Reagent water used throughout this study was obtained from a Milli-Q Gradient A10 Elix system (Millipore, Bedford, MA, USA) and was 18.2 MΩ or greater with a total organic carbon (TOC) content less than 5 parts per billion (ppb). Acetonitrile was Fisher Far UV gradient grade (Fisher Scientific, Waltham, MA). All other chemicals used were purchased from Sigma–Aldrich (St.Louis, MO).

2.3. IgG purification

Protein G/A spin plates (Thermo Scientific) were preconditioned with three washes of binding buffer (PBS) at room temperature. Serum samples (50 μL) were diluted with 50 μL binding buffer (PBS) and applied to the Protein G/A plate. The plate assembly was shaken and incubated for 30 min for IgG binding. After incubation, the plate was washed five times with binding buffer to remove non-specifically interacted proteins. IgG was eluted from the Protein G/A plate using 3 × 300 μL elution buffer (0.5 M acetic acid, pH 2.5). Eluates were collected in a 96 deep well plate and immediately neutralized to pH 7.0 with neutralization buffer (1 M ammonium bicarbonate) to maintain the IgG stability.

The purity of the isolated IgGs was assessed using 10% reducing SDS–PAGE in an Xcell SureLock Mini-Cell (Invitrogen, Carlsbad, CA) according to the manufacturer. Precision Plus Protein All Blue Standards (BioRad, Hercules, CA) was used as the molecular weight marker. The gels were run at 50 mA for 45 min and stained with Gel Code Blue staining reagent (Pierce, Rockford, IL). Separation on SDS–PAGE gel confirmed presence of IgG and lack of any co-eluting proteins (data not shown). Therefore, the sample was confirmed to be pure and suitable for structural analysis of oligosaccharide structures.

2.4. Enzymatic N-glycan release and labelling

Purified IgGs were reduced and alkylated before being set into SDS–PAGE gel blocks, washed and digested with PNGaseF (Prozyme, Hayward, CA, USA) for 16 hours as previously described by Royle et al.[7]

The eluted glycans were fluorescently derivatized via reductive amination with either 2-AB with sodium cyanoborohydride in 30% v/v acetic acid in DMSO at 65 °C for two hours for UPLC-fluorescence studies (both HILIC and RP) or APTS in 15% v/v acetic acid and 1 M sodium cyanoborohydride in tetrahydrofuran at 37 °C overnight for CE-LIF investigations. In both instances the labelling reaction was quenched by the addition of water to yield a final volume of 100 μL. 900 μL of acetonitrile was then added to the reaction vial with subsequent excess fluorophore removal by HILIC phase pipette tips (PhyNexus, San Jose, CA, USA) using an adaptation of the method of Olajos et al.[31] Exoglycosidase digestions were performed using a modified method of Royle et al.[32] N-Glycan nomenclature and symbolic representations used throughout are as previously described by Harvey et al.[33]

2.5. UPLC-fluorescence HILIC N-glycan profiling

2-AB derivatized N-glycans were separated by ultra-performance liquid chromatography (UPLC) with fluorescence detection on a Waters Acquity™ UPLC H-Class instrument consisting of a binary solvent manager, sample manager and fluorescence

detector under the control of Empower 3 chromatography workstation software (Waters, Milford, MA, USA). The HILIC separations were performed using Waters BEH Glycan column, 150 × 2.1 mm i.d., 1.7 μm BEH particles, using a linear gradient of 70–53% acetonitrile at 0.56 mL/min in 16.5 min. Solvent A was 50 mM formic acid which was adjusted to pH 4.4 with ammonia solution and Solvent B was acetonitrile. An injection volume of 20 μL sample prepared in 80% v/v acetonitrile was used throughout. Samples were maintained at 5 °C prior to injection and the separation temperature was 40 °C. The fluorescence detection excitation/emission wavelengths were λ_{ex} = 330 nm and λ_{em} = 420 nm, respectively.

2.6. UPLC-fluorescence RP N-glycan profiling

2-AB derivatized N-glycans were separated by reversed phase using a Waters T3 C18 column, 150 × 2.1 mm i.d., 1.7 μm HSS particles. The buffers used were water with 0.1% formic acid (A) and acetonitrile with 0.1% formic acid (B). The separation was carried out with an initial isocratic separation of 97.5% A held for 5 min. The % A was reduced to 95.5% over 1 min, and then separation was carried out on a shallow gradient to 95% A over 15 min. The sample was prepared in an injection volume of 20 μL in 100% v/v water. The samples were maintained at 5 °C prior to injection and with a separation temperature of 65 °C. The fluorescence detection excitation/emission wavelengths were λ_{ex} = 330 nm and λ_{em} = 420 nm, respectively. Retention times were converted into arabinose unit (AU) values by time based standardization against an arabinose ladder. The arabinose ladder was prepared by acidic hydrolysis of linear arabinan (Megazyme, Bray, Ireland), spiked with arabinose and the 2-mer to 9-mer arabinose sugars chains (Megazyme, Bray, Ireland).

2.7. CE-LIF N-glycan profiling

Capillary electrophoresis separations of APTS labelled N-glycans were performed on a Beckman PA800 Plus Pharmaceutical Analysis System under the control of 32 Karat software, version 9.0 (Beckman Coulter, Brea, CA, USA) using a N-CHO neutral coated capillary, 360 μm O.D., 50 μm I.D. Unless otherwise stated the total capillary length was 60 cm with a 50 cm effective separation length from the injection to the detector. The instrument was equipped with a 3 mW 488 nm solid state laser and a 520 nm cut off filter for laser induced fluorescence detection. For all experiments a commercially available carbohydrate separation buffer was used (Beckman Coulter) at a separation temperature of 25 °C and using an applied potential of −30 kV, (500 Vcm^{-1}), reversed polarity. Prior to use, the capillary was conditioned by subsequent rinsing with water and carbohydrate separation buffer for 10 min at 30 psi. In order to avoid any possible carryover, the capillary was also rinsed with buffer for 5 min at 30 psi between injections. To improve precision, two bracketing standards were used, APTS labelled maltose as the lower and 2-aminoacridone labelled glucuronic acid (2-AMAC GA) as the upper bracket. Samples were injected hydrodynamically at 1 psi for 5 s. Migration times were converted to relative migration times using the bracketing standard boundaries. These normalized migration times were subsequently converted to GU values using a fifth order time based standardization against a maltooligosaccharide ladder (Grain Processing Corporation, Muscatine, IA, USA).

3. Results

3.1. Analysis of IgG glycosylation using different techniques

The strategy for the analysis of N-glycans from IgG is shown in Figure 1. The total IgG was purified from serum using Protein G (human, equine, bovine, ovine) or Protein A (canine, feline) resin, followed by removal of N-glycans by PNGaseF after immobilization in gel plugs. Protein A binds to the Fc portion of the IgG molecule, while Protein G preferentially binds to the Fc portion but also binds the Fab region.[34] The selection of Protein G or Protein A was based on the manufacturer guidelines indicating affinity to different IgG subclasses. The separation of the glycans by various methods yielded different profiles; however, the % abundance of structures obtained by CE-LIF and HILIC–UPLC were similar, whereas the analysis by RP–UPLC was difficult to compare as the structures were separated by classes of glycans where many structures co-eluted. As well, the abundance of sialylated or charged structures in RP–UPLC was not determined due to the fast elution of these structures with the mobile front. The separation time used for each technique was based on optimized conditions to allow for high throughput separation of multiple samples with good resolution. The Oxford notation system has been used to represent N-linked glycan composition and structure (Fig. 2).[33] We will discuss the particular characteristics for each method in the subsequent sections.

3.1.1. Analysis of IgG glycosylation by HILIC–UPLC

HILIC–UPLC separations were performed over 20 min, with the neutral smaller structures eluting first, and the large and charged structures eluting later in the profile (Fig. 3A). The human IgG glycan profile yielded peaks eluting between GU 5 and 10 with major glycan structures eluting at GU 5.88; 6.70; 7.63, and 8.79 (Table 1). From exoglycosidase digestion results (not shown) we identified these glycans as FA2, FA2G1 and FA2G1′, FA2G2 and FA2G2S1 structures. The largest structure possible on human IgG is FA2BG2S2, with two *N*-acetylneuraminic acids (Neu5Ac).

The species specific variation of IgG glycans isolated from a pool of serum from 6 different species is shown in Table 2 (HILIC–UPLC) (CE is not shown as the abundance of each glycan is similar to the results obtained by HILIC–UPLC). For simplicity, peaks that were less than 0.5% relative abundance were not included in the table. The table shows that there are over 50 structures present in the IgG glycans from different mammal species. In humans this is limited to 36 structures. The greater variation observed between non-human species is due to the presence of *N*-glycolylneuraminic acid (Neu5Gc) and larger proportions of bisected structures. As well, the presence of structures containing terminal alpha-linked galactose residues was detected. However, the individual structures containing alpha-linked galactose were less than 0.5% abundant of the total glycan pool. Thus we will not focus on these structures here. Consequently, the profile of the mammal IgG glycans from serum yielded a profile different than that of human (Fig. 3). The major glycans from bovine IgG were fucosylated, with over 80% of glycans consisting of a combination of FA2 (11.9%), FA2G1 (FA2[6]G1 and FA2[3]G1; 9.1% and 19.6%, respectively), and FA2G2 (24.4%). There were roughly 20% bisected biantennary glycans also identified within the profile. Most IgGs isolated from the different mammal species showed some sialylation (*N*-acetyl and *N*-glycolyl neuraminic acid); however, in most species these structures comprised less than 5% of the overall glycan pool, with the exception of FA2G2S1 (α2,6) in human (9.8%) and feline (5.9%) and a disialylated A2G2S2 or FA2BG2Sg1 in the feline IgG (6.8%). Some structures coeluted in the same peak, as their affinity to the column was similar and the elution time allocated was not sufficient to allow for complete separation.

Ovine IgG glycans contained a high percentage of bisected biantennary structures (>60%) of which >40% were fucosylated (Table 2). The majority of structures eluted between GU 5 and 8, and over 85% consisted of neutral non-sialylated structures. The FA2 structure dominated in both the canine and equine IgG glycan profiles (over 50%). In feline, there was over 1% of A1 structure, compared

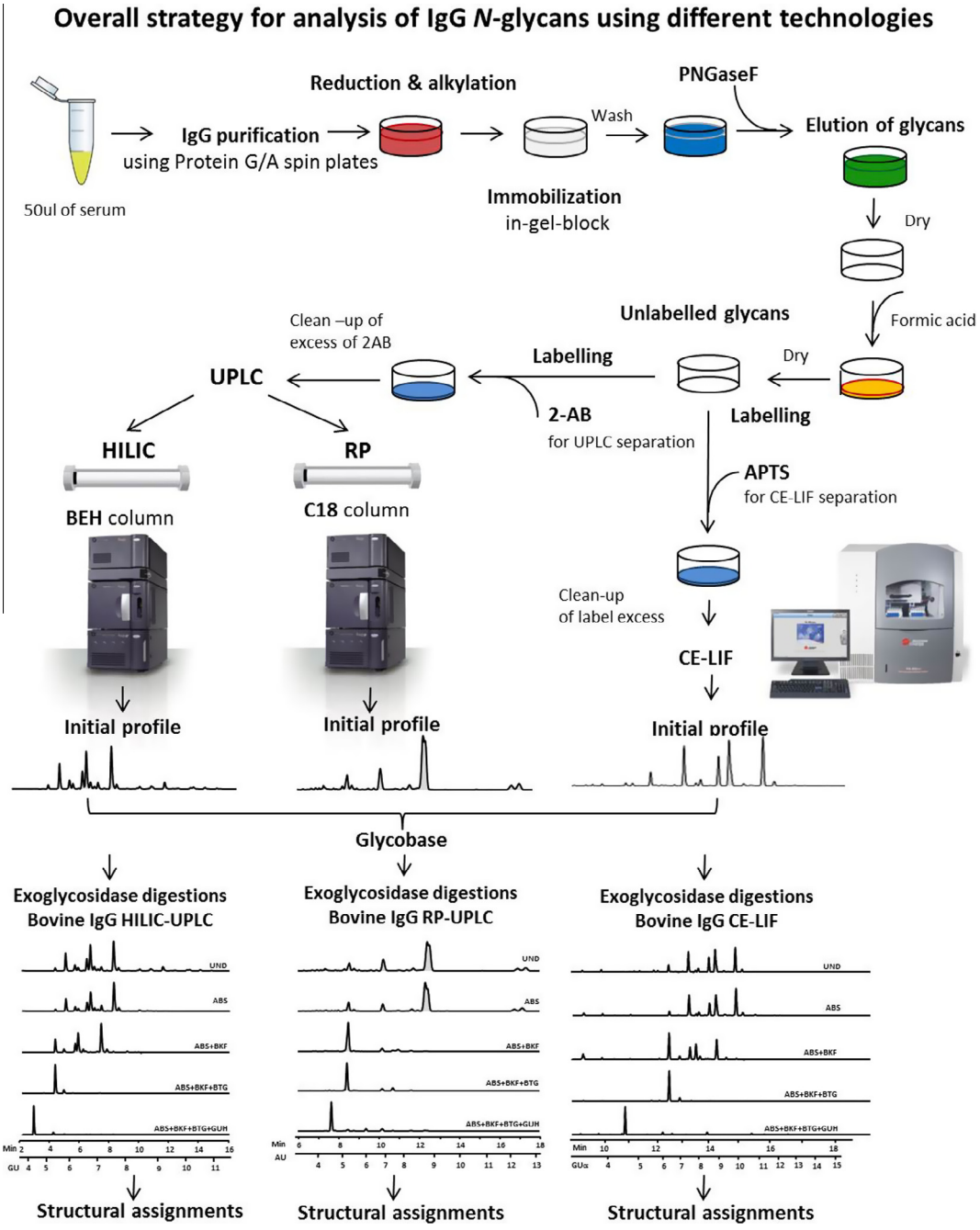

Figure 1. Overall strategy for analysis of IgG N-glycans using HILIC–UPLC, RP-UPLC and CE-LIF separation techniques. This strategy has been applied to analysis of IgG samples from different species; as an example, the profiles of bovine IgGs are presented here.

to other species where this structure was present in negligible amounts. Equine IgG contained more A2G0, FA2[6]G1 and FA2[3]G1 glycans than canine IgG glycans. There were also higher levels of FA2G[6/3] 1 within the equine IgG profiles compared to the canine profiles where the A2 structure was the second most abundant structure. An interesting glycoprofile was generated from feline IgG, which had a highly distributed pattern. The greatest amount of *N*-glycan present in feline profile was A2 (25%) followed by FA2 (17%) while more complex structures were less abundant.

The structural assignments of IgG N-glycans from each mammal were confirmed by digestions using an exoglycosidase enzyme array. *Arthrobacter ureafaciens* sialidase—released α2-6, 3 and 8 linked non-reducing terminal sialic acids (ABS); bovine kidney alpha-fucosidase—released α1-2 and α1-6 linked non-reducing terminal fucose residues more efficiently than α1-3 and 4 linked fucose (BKF); Bovine testes beta-galactosidase hydrolysed non-reducing terminal β1-4 and β1-3 linked galactose (BTG); Hexosaminidase cloned from *Streptococcus pneumoniae* expressed in *Escherichia* coli released GlcNAc residues but not a bisecting GlcNAc linked to Man (GUH). An enzymatic digestion panel for bovine IgG N-glycans is shown in Figure 4A. The original profile consisted of 18 major peaks. After ABS digestion, FA2G2S2 structure with GU 10, digests to an FA2G2 structure with a GU value of 7.63. The removal of two sialic acids resulted in a shift of 2.37 GU value. The fucosidase digestions resolved much of the complexity, where there were four major peaks after the digestion step; A2, A2G1 (with galactose on the 3- or 6-arm) and A2G2. After galactosidase

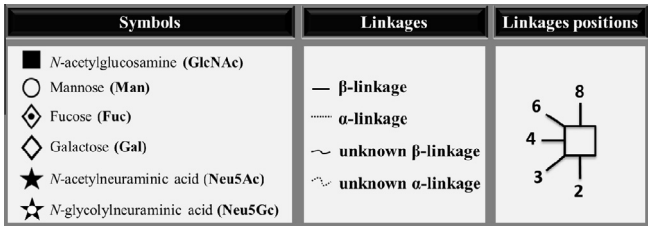

Figure 2. Structural symbols for the N-glycans, their linkages and abbreviations used. Briefly, all N-glycans have two core N-acetylglucosamines (GlcNAc) and a trimannosyl core; F at the start of the abbreviation indicates a core fucose linked α1-6 to the core GlcNAc; A[y]a, represents the number a of antenna (GlcNAc) on the trimannosyl core linked to the α1-y mannose arm; B, bisecting GlcNAc linked β1-4 to β1-4 core mannose; Fb after Aa, represents the number b of fucose linked α1-3 to antenna GlcNAc; Gc, represents the number c of galactose linked β1-4 on antenna; S(z)d, represents number d of sialic acids (Neu5Ac) linked α2-z to the galactose, Sg(z)d, represents number d of sialic acids (Neu5Gc) linked α2-z to the galactose. The graphical symbols are used to represent the different sugar residues and linkages between them. Symbols encode the following monosaccharide structures: GlcNAc, filled square; sialic acid (Neu5Ac), filled star; sialic acid (Neu5Gc), filled star with a white dot; galactose, open diamond; fucose, diamond with a dot inside, mannose, open circle; beta linkage, solid line; alpha linkage, dotted line; unknown beta linkage, solid wave; unknown alpha linkage, dotted wave.

digestion only two major peaks appeared identified as A2 and A2B. Finally after hexosaminidase digestions two peaks (M3 and M3B) remained.

3.1.2. IgG glycosylation analysis by RP–UPLC

The RP–UPLC glycan profiles are shown in Figure 3B and the corresponding abundance of each specific group is shown in Table 3. The 2AB-labelled ladder used in RP separation is based on L-arabinose units linked via an α1,5 linkage (arabinose ladder), and structures are assigned an AU value. The groups are classified as follows: (1) fucosylated, (2) fucosylated and bisected, (3) non-fucosylated and (4) non-fucosylated and bisected. High mannose structures were also separated from all other moieties; however, these were not prominent structures in mammal IgGs. Human, bovine, equine and canine IgG glycans possess high percentage of fucosylated non-bisected structures (>65%). Human IgG N-glycans contain mostly fucosylated structures (FA2, FA2G1, FA2G2 and FA2G2S1) as indicated by the major peaks eluted at 7.7 to 7.8 with a minor percentage (about 10%) of fucosylated bisected structures eluting at 11.5 AU. Bovine IgG was separated by RP–UPLC into 4 distinct regions, where the non-fucosylated, non-bisected glycans were eluted (between 3 and 6 AU), bisected non-fucosylated bisected glycans were eluted between 6 and 7 AU, fucosylated glycans eluted between 7 and 8 AU, and finally fucosylated bisected glycans eluted after 11 AU. Although the abundance of fucosylated non-bisected structures was similar to that of humans, the amount of non-bisected non-fucosylated structures was slightly higher in bovine IgG. The separation of fucosylated, bisected glycans by RP-UPLC gave a clear differentiation in profiles between bovine and ovine IgG glycans that was not evident by the other techniques examinated. Over 40% of fucosylated bisected glycans were present in the ovine IgG glycan sample. The separation of the non-fucosylated, nonbisected glycans (A2G0, A2G1, A2G2) was particularly apparent in ovine and feline IgG glycan profiles, as these structures consisted of 12.9% and 28.9% of the overall profile, respectively. Both equine and canine IgG glycans yielded similar profiles as previously shown by HILIC–UPLC with the major peaks consisting of fucosylated structures (FA2). The relative abundance of the non-fucosylated and non-bisected, non-fucosylated bisected and fucosylated bisected were similar for these species. Feline IgG glycans had a higher percentage of non-fucosylated bisected structures than the other species investigated.

The RP–UPLC separation of exoglycosidase digested glycans did not yield specific digestion profiles as in the case of

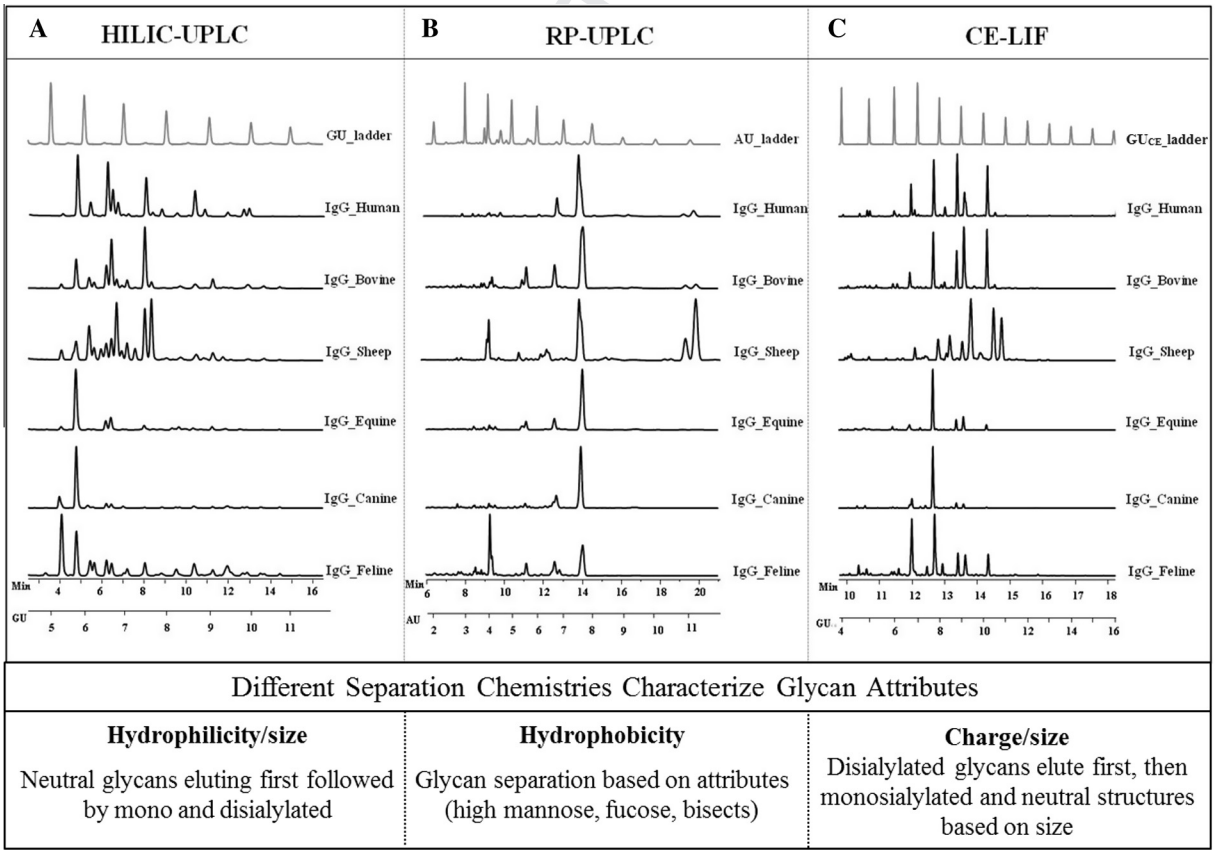

Figure 3. N-glycosylation profiles of human, bovine, ovine, equine, canine and feline IgG using HILIC–UPLC (A), RP–UPLC, (B) and CE-LIF (C).

Table 1
Summary of N-glycan structural composition determined for human IgG

	Structure	Cartoon	GU (HILIC–UPLC)	AU (RP–UPLC)	GU_{CE} (CE-LIF)
1	F(6)A1	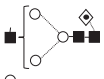	5.32	4.76	F(6)A1[6]: 6.65 F(6)A1[3]: 7.01
2	A2		5.41	4.07	6.67
3	A2B		5.78	6.35	7.20
4	F(6)A2		5.88	7.72	7.69
5	M5		5.92	2.71	6.75
6	F(6)A2B		6.24	11.22	8.20
7	A2[6]G1		6.25	4.07	7.74
8	A2[3]G1		6.38	4.07	8.04
9	A2B[6]G1		6.54	6.51	8.26
10	A2B[3]G1		6.71	6.51	8.55
11	F(6)A2[6]G1		6.70	7.80	8.75
12	F(6)A2[3]G1		6.84	7.80	9.08
13	F(6)A2B[6]G1		6.94	11.50	9.14
14	F(6)A2B[3]G1		7.07	11.50	9.55
15	A2G2	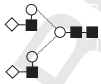	7.21	4.07	9.12
16	A2BG2		7.36	6.61	9.62
17	F(6)A2G2		7.63	7.80	10.13
18	F(6)A2BG2	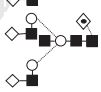	7.77	11.50	10.48
19	F(6)A1G1S1	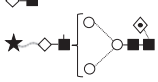	7.77	X	F(6)A1[6]G1S1: 5.08 F(6)A1[3]G1S1: 5.24
20	A2[6]G1S1	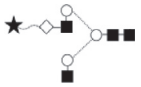	7.48	X	5.24
21	A2[3]G1S1		7.62	X	5.39
22	A2B[6]G1S1		7.78	X	5.65

Table 1 (*continued*)

	Structure	Cartoon	GU (HILIC–UPLC)	AU (RP–UPLC)	GU_{CE} (CE-LIF)
23	A2B[3]G1S1	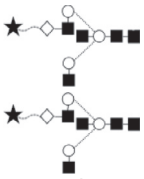	7.93	X	5.99
24	M4A1G1S1		7.90	X	X*
25	F(6)A2[6]G1S1	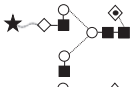	7.90	X	5.81
26	F(6)A2[3]G1S1	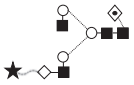	8.03	X	5.91
27	F(6)A2B[6]G1S1	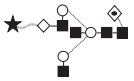	8.13	X	6.00
28	A2G2S1	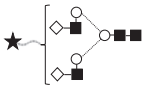	8.38	X	6.11
29	F(6)A2B[3]G1S1	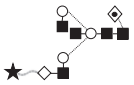	8.38	X	6.13
30	A2BG2S1	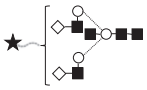	8.61	X	6.37
31	F(6)A2G2S1	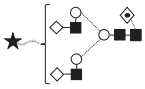	8.79	X	6.63
32	F(6)A2BG2S1	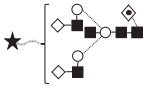	9.00	X	6.79
33	A2G2S2	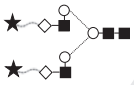	9.58	X	4.54
34	A2BG2S2		9.74	X	4.70
35	F(6)A2G2S2		10.00	X	4.83
36	F(6)A2BG2S2		10.12	X	4.92

All N-glycans are reported with corresponding glucose units (GU), arabinose units (AU) and glucose units (capillary electrophoresis) (GU_{CE}) values for IgG *N*-glycan structures from human IgG. Structures are given in the Oxford notation[32] and structural symbols for the N-glycans, their linkages and abbreviations are presented in Figure 2.

HILIC-separations. As the separation occurs by 'classes', the digestion of specific terminal sugars yielded a change in the group type. Moreover, the peaks did not shift with constant AU value, as the digestion of sugars resulted in changes of hydrophobicity. Figure 4B shows the separation of the exoglycosidase digestion products of bovine IgGs. The ABS digestion resulted in a minor change in the earlier eluting peaks; and an AU increase in the A2G2 peak to 4.07. A major change in the profile occurred after BKF digestion, when the fucosylated peak shifted from AU 7.8 to AU 4.7. The peak at AU 7.8 prior to BKF digestions contained two unresolved peaks (shoulder) indicating that this peak contained more than one structure. Based on HILIC and CE-LIF analysis, this peak probably contained FA2, FA2G1 and FA2G2 structures. There were also changes in the shifts of some minor peaks in the AU range of 6.25–6.5 corresponding to bisected nonfucosylated structures (A2BG0, A2BG1 and A2BG2) after galactosidase digestions. After the application of the full digestion panel, only the A2 structure remained (AU = 3.0).

3.1.3. Analysis of IgG glycosylation by CE-LIF

CE traces of the IgG glycans from different species are shown in Figure 3C. Full migration required over 30 min; however, the majority of glycans migrated through the detection window between 10 and 18 min. The separation yielded very narrow individual peaks, indicating complete resolution of the isomers. The separation trace was similar to the HILIC separation profile; however, some peaks were more prominent in the HILIC traces compared to the CE traces. In the HILIC traces some of the larger peaks were composed of more than one structures, as in the case

Table 2
Relative abundances of the IgG glycan structures from the six mammalian species, as determined by HILIC–UPLC[b] analysis

	GU	Abundance (% area)					
		Human	Bovine	Ovine	Equine	Canine	Feline
A1	4.8						1.2
A2	5.4	0.7	1.7	2.6	2.8	12.5	23.3
A2B	5.8			1.0			
F(6)A2	5.9	20.6	11.9	5.5	50.8	56.2	16.3
F(6)A2B	6.2	5.3	4.8	9.5		3.3	6.1
A2[6]G1							
F(6)A2B/A2[3]G1	6.4		2.5	3.2	0.7	1.2	5.1
A2B[6]G1	6.5			3.0			
A2B[3]G1							
F(6)A2[6]G1	6.6	18.1	9.1	4.7	7.6	4.2	5.7
F(6)A2[3]G1	6.8	9.2	19.6	5.5	11.1	4.1	4.7
F(6)A2B[6]G1	6.9	4.8	3.8	14.9			
F(6)A2B[3]G1	7.0	0.6	1.5	2.4	0.7	2.0	0.9
F(6)A2B[3]G1/A2G2	7.1	0.8	3.4	4.5			2.8
A2BG2	7.3			3.1			
F(6)A2G2	7.5	13.7	24.4	13.1	5.5	0.8	5.4
F(6)A2BG2	7.6	1.6	2.8	15.8	1.3		0.5
F(6)A1G1S1							
A2[6]G1S1							
A2[3]G1S1							
A2B[6]G1S1							
A2B[3]G1S1							
F(6)A2[3]G1S1	7.9	2.9		0.9	1.2	1.1	1.6
F(6)A2B[6]G1S1							
A2[6]G2Sg1[a]							
A2[3]G1Sg1[a]							
A2G2S1	8.0	1.6			2.5	0.9	3.3
F(6)A2B[3]G1S1							
F(6)A2G2S1(a2,3)							
A2G2Sg1[a]							
F(6)A2G2Sg1 (α2,3)[a]	8.2		1.4	1.8	3.1	0.9	
A2BG2S1	8.6				1.7		
F(6)A2G2S1 (α2,6)	8.8	9.8	2.9	2.5	2.2	2.6	5.9
F(6)A2BG2S1	9.0	2.8		1.1	1.1		0.7
F(6)A2G2Sg1[a]	9.1		4.3	2.5	3.0	1.7	2.8
A2G2S2(α2,6/α2,6)	9.6	1.9	0.8	1.1	2.0	3.4	6.8
F(6)A2BG2Sg1[a]							
A2BG2S2	9.7					0.6	1.0
F(6)A2G2S2	10.0	2.6			1.7	2.1	2.4
A2G2S1Sg1[a]	10.1	3.2	2.7	0.6		1.4	1.6
A2G2Sg2[a]							
F(6)A2G2Sg2 (α2,3/α2,3)[a]							
F(6)A2BG2Sg2 (α2,3/α2,3)[a]							
F(6)A2BG2S2							
A2G2Sg2 (α2,6/α2,6)[a]	10.3		1.5	0.8	0.6		1.0
F(6)A2G2S1Sg1 (α2,6/α2,6)[a]							
F(6)A2G2Sg2 (α2,3/α2,6)[a]							
F(6)A2BG2Sg2 (α2,3/α2,6)[a]							
F(6)A2BG2Sg2 (α2,6/α2,6)[a]	10.8		0.8		0.6	1.1	0.9

[a] *N*-Glycolyl neuraminic acid containing structures—not present in human IgG glycans.
[b] Relative abundances as determined by CE were similar to that obtained in HILIC; However, there was some ambiguity between *N*-acetyl and *N*-glycolyl neuraminic acid containing structures.

of the peak GU = 6.25 (A2[6]G1 and FA2B) in the human IgG, however, in the CE electropherogram these two structures were well resolved having GU_{CE} of 8.20 and 7.74, respectively.

The CE-LIF exoglycosidase digestion patterns (Fig. 4C) were similar to HILIC–UPLC digestions. Since the peaks eluting between 4 and 7 GU_{CE} shifted to corresponding peaks of A2, FA2, A2G1, FA2G1, A2G2 and FA2G2 after ABS digestions, these peaks were identified as sialylated. A digestion profile panel shows similar patterns to the HILIC–UPLC chromatograms albeit their digested product of an enzymatic reaction shifted to smaller GU values. Apart from the sialic acid containing structures, the digestions of the other terminal sugars yielded predictable GU shifts.

4. Discussion

In this paper we compared three separation methods to investigate the overall IgG glycosylation profile of various mammalian species (human, bovine, ovine, equine, canine and feline). The comparison of the separation methods included HILIC–UPLC, RP–UPLC and CE-LIF. The methods utilized different separation principles, and thus enabled mostly orthogonal analysis of the different sugar structures.

Each method has different requirements in respect to sample preparation, necessary equipment and separation time but offers quasi orthogonal information about the glycans present. All aspects discussed below should be taken into account when selecting the technique of choice. Comparison of the data obtained for human IgG by each method is shown in Table 1. The percentage abundance of N-glycan structures calculated from each method is similar, suggesting that the separation and detection of glycans by each method do not have structural selectivity. This is especially important in the case of APTS labelling in CE-LIF glycan separation technique, as published data have indicated the importance of labelling under optimized conditions so that sialylation or other

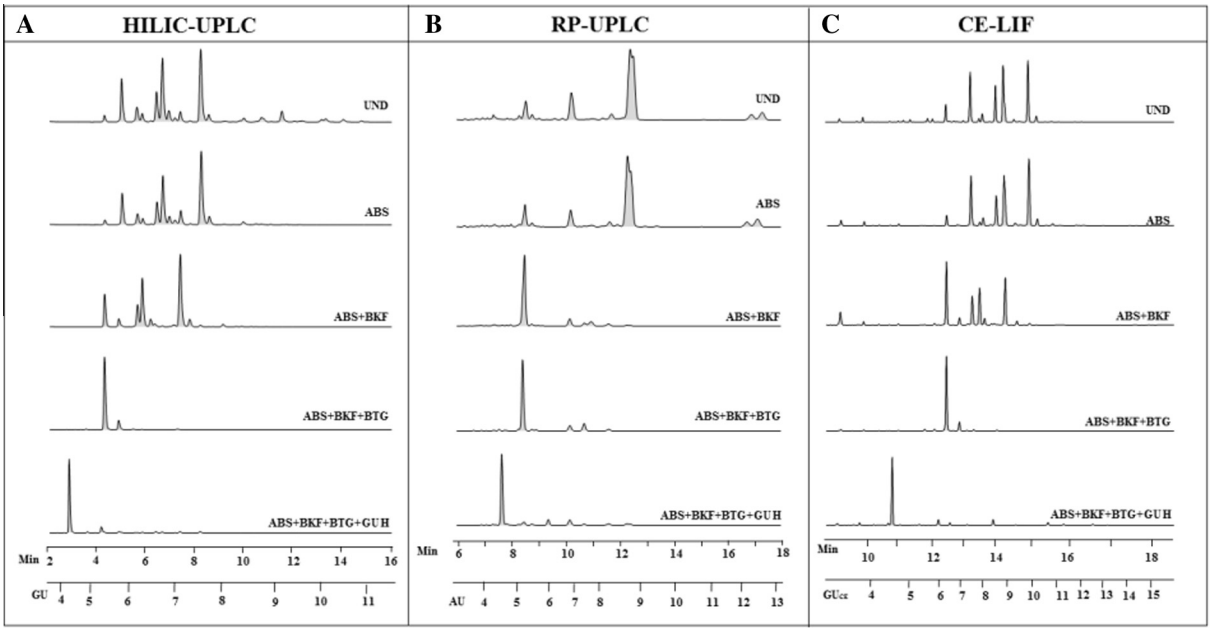

Figure 4. Exoglycosidase panel digestions of bovine IgG glycans separated by HILIC–UPLC (A), RP–UPLC (B) and CE-LIF (C). The exoglycosidase panel consisted of *Arthrobacter ureafaciens* sialidase (ABS), Bovine kidney alpha-fucosidase (BKF), Bovine testes beta-galactosidase (BTG) and hexosaminidase (GUH), with sequential additions.

Table 3
Relative abundances of IgG glycan classes from the six mammalian species, as determined by RP-UPLC analysis

	% Abundance					
	Human	Bovine	Ovine	Equine	Canine	Feline
'Classes' of glycans						
Fucosylated & non-bisected	68.3	68.6	14.5	75.3	74.3	21.1
Fucosylated & bisected	10.4	12.0	46.3	3.2	1.1	6.3
Non-fucosylated & non-bisected	5.5	8.7	12.9	8.2	7.0	28.9
Non-fucosylated & bisected	15.8	10.7	26.3	13.3	17.6	43.7

labile sugar containing structures are not mis-represented.[35] As we report on the separation of IgG glycans, this is less crucial, as sialylation is quite low, representing only about up to 5% of the total glycan pool from each species. The detection limit of APTS-labelled glycans by CE-LIF is estimated to be 0.4 nM using a 3 mW 488 nm argon-ion laser,[36] which is slightly less sensitive than HILIC–UPLC; however, the injection volume of the latter is on average 3 orders of magnitude higher than in CE. CE-LIF allows for the separation of all IgG glycans in 8 min based on the conditions applied in this paper with the overall separation time just over 20 min. The use of CE-LIF as a method of glycan separation of monoclonal antibodies has been thoroughly discussed previously and the separation of glycans by this method for the elucidation of structural isomers has proven effective.[12,31,37] However, as these CE-LIF studies in the literature have been compared to separation of glycans by HILIC–UPLC, the separation of structural isomers will not be discussed further here. Besides the CE system used in this study, other commercially available general purpose CE units can also be used in a similar manner.[38] Special capillary based systems, such as DNA sequencers, require medium to high viscosity gels to run the instruments, thus only allow electrokinetic injection.[39,40] Unfortunately, this causes sample introduction bias and concomitantly alters the resulting profile.

The separation method for glycan analysis by RP–UPLC and HILIC–UPLC, used in this paper, occurred over 15 and 18 min, respectively. The separation of the glycans in RP–LC separation mode occurs in well-defined zones such as high-mannose structures eluting first, followed by biantennary complex structures and finally the fucosylated complex structures. RP separation groups are based on the hydrophobicity; thus major differences in glycan structures can be easily visualized, that is the large proportion of bisected glycans in ovine. In contrast to HILIC separation, RP data analysis has greater difficulty in assigning individual glycan structures. The shift in AU values of digested glycan structures run on RP–UPLC is not predictable based on sequential removal of terminal sugar residues. Since the sugar structures are separated based on the hydrophobicity of the glycan and the fluorescent tag,[41] the removal of terminal sugars may have an unpredictable influence on the shift of glycans after digestion. With the HILIC method one can expect reproducible shifts in the range of 0.4 to 1.15 (and 0.15 to 0.2 for bisecting GlcNAcs), for exoglycosidase digested glycans depending on the sugars removed. In case of combined sialidase (ABS) and fucosidase (BKF) digestions for example, the peak at 7.8 shifted to 4.07 AU as shown in Figure 4B.

Sialylated glycans could not be identified by RP–UPLC analyses, as these structures are highly hydrophilic and elute from the column with the void. This method can therefore only be used for the analysis of non-charged structures. RP-UPLC glycan separation could be applied in the biotechnology industry for the analysis of N-glycans from CHO produced monoclonal antibodies where sialylation is generally less than 2%. RP–UPLC may be highly applicable for samples containing structures with bisecting GlcNAc or high mannose structures as glycans containing these features elute in separate groups. It must be noted however that many structures have a tendency to co-elute, such as the fucosylated A2, fucosylated A2G1 and fucosylated A2G2 with this method. In general, RP–UPLC of glycans is not as efficient as HILIC–UPLC or CE-LIF and RP–UPLC data analysis has greater difficulty in assigning individual glycan structures, but it could be used as a complementary tool for example, in 2D separations to resolve structures that possibly co-elute in HILIC.[9]

Table 4
Advantages and disadvantages of methods presented in this article

Method	HILIC–UPLC	RP–UPLC	CE-LIF
Information			
Order of erutins structures	From simple to more complex	Based on structural features and hydrophobicity	From simple to more complex, with sialylated first
Comparison to standard	Yes	Yes	Yes
Oligosaccharide ladder	Dextran	Arabinose	Maltodextrin
Availability of database	Yes	No*	No*
Number of structures in the database	600	—	—
Obtained information	Glycan profiling; structure; linkage assignments	Glycan profiling; structure	Glycan profiling; structure; linkage assignments
Exoglycosidase digestions	Predictable	Not-predictable	Predictable
Technical aspects			
Relative quantification	Yes	Yes	Yes
Sample volume	10–25 μL	25 μL	<1 μL
Resolution	High	Medium	High
Mobile Phase	50 mM Ammonium Formate/Acetonitrile	Ammonium Formate/1% Formic acid	Proprietary Carbohydrate buffer
Stationery Phase	BEH column	C18 column	CHO coated capillary
Operational constraints			
Labelling	2-AB	2-AB	APTS
Separation time	10–30 min	10–30 min	20 min
Data analysis	Medium	Medium	Medium
User expertise	3–6 months	3–6 months	3–6 months
High-throughput capability	Yes	Yes	Yes

* The developments of RP- and CE-LIF databases are ongoing.

The glycan peaks in RP mode generally have shoulders, and are not resolved completely. Although this can be an issue with all the investigated methods, this is particularly prevalent in RP, but can be optimized by using different packing materials or varying elution conditions (i.e., gradients). However, as the buffer gradient in RP-UPLC separations is quite shallow, modification is challenging. Alternate packing materials are under current investigation and need to be tested for increased resolution of complex glycans. Extensive research efforts have been put into the understanding of the fundamental retention behaviour of analytes when separated by columns comprised of various packing materials; in particular the separation by monolithic silica,[42,43] or silanol silica.[44] For the analysis of larger complex glycans RP separation would be most efficient especially when coupled with mass spectrometry.[9,41,45,46] Such coupling however, increases analysis times and requires further expertise.

Table 1 shows the different glucose units using a dextran ladder (GU), arabinose ladder (AU) and maltooligosaccharide ladder (GU_{CE}) values of various structures identified from IgG glycans in human. It is important to point out that the values are different between each method; due to the difference in the separation principles. Although the CE and HILIC methods utilize GU values, the ladders used for unit identification are composed of a differently linked glucose polymers (α1-4 and α1-6 linked glucose polymers, respectively). CE separation is based on the charge to hydrodynamic volume ratio of the analyte molecules. Since most carbohydrates are not charged labelling of the glycans with a charged fluorophore or chromophore is necessary for their electric field mediated separation. The development of sugar unit databases has been the focus of several leading laboratories over the past years. Glycobase 3.2 comprises the data of over 600 N-glycan structures separated by HILIC–HPLC and HILIC–UPLC (http://glycobase.nibrt.ie). The developments of RP- and CE-LIF databases are ongoing. The differences between the three methods investigated in this study are outlined in Table 4.

HILIC or CE are generally the first methods of choice, as plenty of information is available for data interpretation from the respective databases. The separation of glycans by HILIC requires an UPLC or HPLC. The latter is often available in most laboratories thus enabling relatively affordable analysis. On UPLC columns analytical separations for glycan samples are now reduced to only 30 minutes or less, and the techniques are continually improving to accommodate high throughput glycan analysis needs. Sample preparation protocols were labour-intensive but with the recently developed robotic platforms for IgG N-glycan analysis the throughput capabilities are much greater [47–49] and based on 96 or 384 well plates. General interest in glycan analysis continues to grow as more life science researchers realize its importance in many biological processes. With growing interest and developed technologies, glycomic analysis should become more common in academic, industrial as well as healthcare centres.

The HILIC–UPLC- and CE-LIF based separations also enable glycoprofiling with position/linkage assignments when used in combination with exoglycosidase digestion arrays. For each separation technique the enzyme array yields different traces; in the case of HILIC and RP UPLC, due to the interaction of the glycans with the stationary phase, and in the case of CE-LIF, the change in the overall charge to mass ratio imparted upon the glycans. While exoglycosidase digestion results are predictable in HILIC- and CE-LIF; RP-separation is unable to deliver linkage information due to the lack of resolving power. Another drawback of RP is the presence of non-glycan compounds (contaminant) peaks interfering with glycans of AU values from 6 to 7.5. These contaminants may originate from the glycoprotein itself during the release process. In addition, charged glycans elute with the solvent front, and thus could not be identified. While HILIC- and CE-LIF analysis enable relative and absolute quantification of individual structures, RP- separation enables relative quantification of groups of glycans, due to structural co-elution. HILIC– and RP–UPLC analysis of glycans requires a label with a minor function to mediate HILIC–UPLC separation, and a major function in RP separation.

Other methods of analyses, such as mass spectrometric methods using fragmentation, can be used to elucidate the glycosylation differences between the IgG from different species. Sequence information can be generated by fragmentation, but linkage position type and position is less straightforward. The use of exoglycosidase enzymes may be possible; however, due to the introduction of salts in the reaction buffer samples require extensive sample clean up or ionization efficiency maybe compromised. For linkage analysis, for instance using permethylation or exoglycosidase digestions, more

Table 5
Structures with >5% abundance in mammalian IgGs

Nomenclature	Structure	% Abundance
Human		
F(6)A2		20.6
A2[6]G1 or F(6)A2B	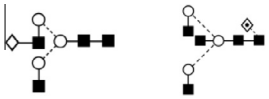	5.3
F(6)A2[6]G1	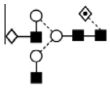	18.1
F(6)A2[3]G1	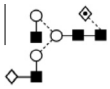	9.2
F(6)A2G2	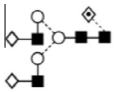	13.7
F(6)A2G2S(6)1	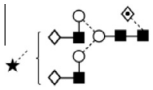	9.8
Bovine		
F(6)A2		11.9
F(6)A2[6]G1	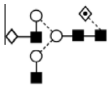	9.1
F(6)A2[3]G1	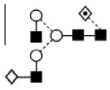	19.6
F(6)A2G2	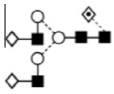	24.4
Ovine		
F(6)A2	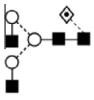	5.5
F(6)A2B	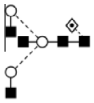	9.5
F(6)A2[3]G1	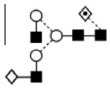	5.5
F(6)A2B[6]G1	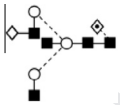	14.9
F(6)A2G2		13.1
F(6)A2BG2	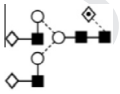	15.8
Equine		
F(6)A2		50.8
F(6)A2[6]G1	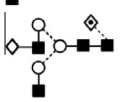	7.6

Table 5 (*continued*)

Nomenclature	Structure	% Abundance
F(6)A2[3]G1	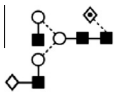	11.1
F(6)A2G2	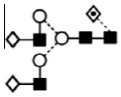	5.5
Canine		
A2		12.5
F(6)A2		56.2
Feline		
A2		23.3
F(6)A2	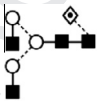	16.3
F(6)A2B/A2[6]G1	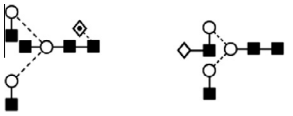	6.1
F(6)A2B/A2[3]G1	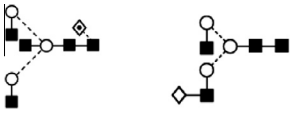	5.1
F(6)A2[6]G1	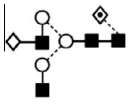	5.7
F(6)A2G2	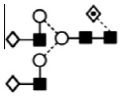	5.4
F(6)A2G2S1	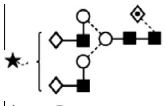	5.9
A2G2S(6,6)2/ F(6)A2G2Sg(3)1	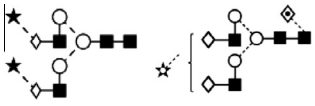	6.8

glycan material would be necessary, due to sample preparation losses by either technique.

Our analysis of the IgG glycans from various mammalian species highlights the benefits of using various methods for analysis and indicated high structural variation in the mammalian IgG glycans, while being consistent with previously published data.[50] Raju and colleagues reported on the glycosylation differences from 13 different species using CE-LIF and MALDI-TOF-MS analyses.[50] Their results indicated species-specific variation in core fucosylation, terminal galactosylation and bisecting GlcNAc residues. Another study compared the IgG glycosylation from 11 species, porcine, equine, bovine, goat, ovine, canine, rabbit, guinea-pig and rat, by microsequencing and lectin affinity chromatography.[51] The IgG glycans identified by Hamako et al.[51] consisted of biantennary complex-type oligosaccharides containing 0–2 sialic acid residue(s), where more than 70% of the oligosaccharides were neutral

and fucosylated trimannosyl core structures. The bisecting residue was absent in equine IgGs. In agreement with our results, large quantities of agalactosylated oligosaccharides were identified in equine and canine IgGs.

The techniques discussed in this paper resolved glycan structures from the various species. Using these orthogonal methods for the analysis of N-glycans from the IgGs from different species, information regarding the glycan differences in IgGs can be gathered. The most abundant structures from studied species are summarized in Table 5. The HILIC–UPLC is reliable technique that effectively separates and quantitates structures on the basis of both sequence and linkages. The isolation of different classes of N-glycans (highly mannosylated, fucosylated, bisected, fucosylated and bisected) by RP–UPLC offers the separation of IgG N-glycans by group classes. And finally separation by CE-LIF offers separation by the relationship of the charge imposed by the electric field to hydrodynamic volume. In conclusion, these fast and effective separation techniques can be used along with other analytical methodologies to allow for full structural characterization.

Acknowledgements

This work was supported by the Science Foundation Ireland (Reproductive Biology Research Cluster (RBRC) [Grant Number 07/SRC/B1156] and Alimentary Glycoscience Research Cluster (AGRC) [Grant Number 08/SRC/B1393]). European Commission under the Seventh Framework Programme (FP7) EuroGlycoArrays [Grant Number 215536], GlycoHIT [Grant Number 260600], GlycoBioM [Grant Number 259869], HighGlycan [Grant Number 278535] and by Ingabritt and Arne Lundbergs Research Foundation.

BA acknowledges funding from the European Union FP7 GastricGlycoExplorer ITN under Grant Agreement No. 316929. A.G. and A.S.Z. acknowledge the OTKA grant # K-81839 support of the Hungarian Research Council and the MTA-PE Translational Glycomics support of the Hungarian Academy of Sciences. We would also like to thank Michael Garrett from the Veterinary Sciences Clinic at University College Dublin for collecting the mammalian serum and Dr. Simone Albrecht for critical reading of this manuscript.

References

1. Kobata, A. *Biochim. Biophys. Acta (BBA)—Gen. Subj.* **2008**, *1780*, 472–478.
2. Mimura, Y.; Ashton, P. R.; Takahashi, N.; Harvey, D. J.; Jefferis, R. *J. Immunol. Methods* **2007**, *326*, 116–126.
3. Ohtsubo, K.; Marth, J. D. *Cell* **2006**, *126*, 855–867.
4. Hilliard, M.; Struwe, W.; Carta, G.; O'Rourke, J.; McLoughlin, N.; Rudd, P. M.; Qing, Y., 2012.
5. Ahn, J.; Bones, J.; Yu, Y. Q.; Rudd, P. M.; Gilar, M. *J. Chromatogr. B* **2010**, *878*, 403–408.
6. Bones, J.; Mittermayr, S.; O'Donoghue, N.; Guttman, A.; Rudd, P. M. *Anal. Chem.* **2010**, *82*, 10208–10215.
7. Royle, L.; Campbell, M. P.; Radcliffe, C. M.; White, D. M.; Harvey, D. J.; Abrahams, J. L.; Kim, Y.-G.; Henry, G. W.; Shadick, N. A.; Weinblatt, M. E.; Lee, D. M.; Rudd, P. M.; Dwek, R. A. *Anal. Biochem.* **2008**, *376*, 1–12.
8. Vervoort, R.; Debets, A.; Claessens, H.; Cramers, C.; De Jong, G. *J. Chromatogr. A* **2000**, *897*, 1–22.
9. Kurihara, T.; Min, J. Z.; Hirata, A.; Toyo'oka, T.; Inagaki, S. *Biomed. Chromatogr.* **2009**, *23*, 516–523.
10. Ruhaak, L. R.; Hennig, R.; Huhn, C.; Borowiak, M.; Dolhain, R. J.; Deelder, A. M.; Rapp, E.; Wuhrer, M. *J. Proteome Res.* **2010**, *9*, 6655–6664.
11. Szabo, Z.; Guttman, A.; Rejtar, T.; Karger, B. L. *Electrophoresis* **2010**, *31*, 1389–1395.
12. Ma, S.; Nashabeh, W. *Anal. Chem.* **1999**, *71*, 5185–5192.
13. Zamfir, A. D.; Bindila, L.; Lion, N.; Allen, M.; Girault, H. H.; Peter-Katalinic, J. *Electrophoresis* **2005**, *26*, 3650–3673.
14. Kirsch, S.; Bindila, L. *Bioanalysis* **2009**, *1*, 1307–1327.
15. Kosicek, M.; Kirsch, S.; Bene, R.; Trkanjec, Z.; Titlic, M.; Bindila, L.; Peter-Katalinic, J.; Hecimovic, S. *Anal. Bioanal. Chem.* **2010**, *398*, 2929–2937.
16. North, S. J.; Hitchen, P. G.; Haslam, S. M.; Dell, A. *Curr. Opin. Struct. Biol.* **2009**, *19*, 498–506.
17. Zamfir, A.; Vakhrushev, S.; Sterling, A.; Niebel, H. J.; Allen, M.; Peter-Katalinic, J. *Anal. Chem.* **2004**, *76*, 2046–2054.
18. Lundborg, M.; Widmalm, G. *Anal. Chem.* **2011**, *83*, 1514–1517.
19. Barb, A. W.; Prestegard, J. H. *Nat. Chem. Biol.* **2011**, *7*, 147–153.
20. Zauner, G.; Deelder, A. M.; Wuhrer, M. *Electrophoresis* **2011**, *32*, 3456–3466.
21. Marino, K.; Bones, J.; Kattla, J. J.; Rudd, P. M. *Nat. Chem. Biol.* **2010**, *6*, 713–723.
22. Rudd, P. M.; Dwek, R. A. *Curr. Opin. Biotechnol.* **1997**, *8*, 488–497.
23. Domann, P. J.; Pardos-Pardos, A. C.; Fernandes, D. L.; Spencer, D. I. R.; Radcliffe, C. M.; Royle, L.; Dwek, R. A.; Rudd, P. M. *Proteomics* **2007**, *7*, 70–76.
24. Guttman, A.; Chen, F. T.; Evangelista, R. A. *Electrophoresis* **1996**, *17*, 412–417.
25. Briggs, J. B.; Keck, R. G.; Ma, S.; Lau, W.; Jones, A. J. *Anal. Biochem.* **2009**, *389*, 40–51.
26. Chen, F. T.; Evangelista, R. A. *Electrophoresis* **1998**, *19*, 2639–2644.
27. Guttman, A.; Ulfelder, K. W. *J. Chromatogr. A* **1997**, *781*, 547–554.
28. Murray, S.; McKenzie, M.; Butler, R.; Baldwin, S.; Sutton, K.; Batey, I.; Timmerman-Vaughan, G. M. *Anal. Biochem.* **2011**, *413*, 104–113.
29. Mittermayr, S.; Guttman, A. *Electrophoresis* **2012**, *33*, 1000–1007.
30. Campbell, M. P.; Royle, L.; Radcliffe, C. M.; Dwek, R. A.; Rudd, P. M. *Bioinformatics* **2008**, *24*, 1214–1216.
31. Hajols, P. t.; Olajos, M.; Bonn, G. K.; Guttman, A. s. *Anal. Chem.* **2008**, *80*, 4241–4246.
32. Royle, L.; Radcliffe, C. M.; Dwek, R. A.; Rudd, P. M. Detailed Structural Analysis of *N*-glycans Released From Glycoproteins in SDS–PAGE Gel Bands Using HPLC Combined With Exoglycosidase Array Digestions In *Methods in Molecular Biology*; Brockhausen, I., Ed.; Humana Press: Totowa, NJ, 2006; Vol. 347, pp 125–143.
33. Harvey, D. J.; Merry, A. H.; Royle, L. *Proteomics* **2009**, *9*, 3796–3801.
34. Erntell, M.; Myhre, E. B.; Sjöbring, U.; Björck, L. *Mol. Immunol.* **1988**, *25*, 121–126.
35. Chen, F. T. A.; Dobashi, T. S.; Evangelista, R. A. *Glycobiology* **1998**, *8*, 1045–1052.
36. Evangelista, R. A.; Liu, M. S.; Chen, F. T. A. *Anal. Chem.* **1995**, *67*, 2239–2245.
37. Mittermayr, S.; Bones, J.; Doherty, M.; Guttman, A.; Rudd, P. M. *J. Proteome Res.* **2011**, *10*, 3820–3829.
38. Camilleri, P. *Capillary Electrophoresis: Theory and Practice*, 2nd ed.; Taylor & Francis, 1997.
39. Vanderschaeghe, D.; Laroy, W.; Sablon, E.; Halfon, P.; Van Hecke, A.; Delanghe, J.; Callewaert, N. *Mol. Cell. Proteomics* **2009**, *8*, 986–994.
40. Vanderschaeghe, D.; Szekrényes, A. k.; Wenz, C.; Gassmann, M.; Naik, N.; Bynum, M.; Yin, H.; Delanghe, J.; Guttman, A.; Callewaert, N. *Anal. Chem.* **2010**, *82*, 7408–7415.
41. Prater, B. D.; Connelly, H. M.; Qin, Q.; Cockrill, S. L. *Anal. Biochem.* **2009**, *385*, 69–79.
42. El Deeb, S.; Preu, L.; Wätzig, H. *J. Sep. Sci.* **2007**, *30*, 1993–2001.
43. Atia, N. N.; York, P.; Clark, B. J. *J. Sep. Sci.* **2009**, *32*, 931–938.
44. Neue, U. D.; Phoebe, C. H.; Tran, K.; Cheng, Y. F.; Lu, Z. *J. Chromatogr. A* **2001**, *925*, 49–67.
45. Chen, X.; Flynn, G. C. *Anal. Biochem.* **2007**, *370*, 147–161.
46. Melmer, M.; Stangler, T.; Premstaller, A.; Lindner, W. *J. Chromatogr. A* **2011**, *1218*, 118–123.
47. Stöckmann, H.; Adamczyk, B.; Hayes, J.; Rudd, P. M. *Anal. Chem.* **2013**, *85*, 8841–8849.
48. Reusch, D.; Haberger, M.; Selman, M. H. J.; Bulau, P.; Deelder, A. M.; Wuhrer, M.; Engler, N. *Anal. Biochem.* **2013**, *432*, 82–89.
49. Doherty, M.; Bones, J.; McLoughlin, N.; Telford, J. E.; Harmon, B.; DeFelippis, M. R.; Rudd, P. M. *Anal. Biochem.* **2013**, *442*, 10–18.
50. Raju, T. S.; Briggs, J. B.; Borge, S. M.; Jones, A. J. S. *Glycobiology* **2000**, *10*, 477–486 .
51. Hamako, J.; Matsui, T.; Ozeki, Y.; Mizuochi, T.; Titani, K. *Comp. Biochem. Physiol. Part B: Comp. Biochem.* **1993**, *106*, 949–954.